Ann. For. Res. 68(1): 137-154, 2025
https://doi.org/10.15287/afr.2025.4051

ANNALS OF FOREST RESEARCH
www.afrjournal.org

Sentinel-2 and environmental data as predictors of the spatiotemporal dynamics of bark beetle (Coleoptera: Scolytinae) - induced tree mortality in natural spruce forests

Matúš Pivovar[1,2], Pavel Mezei[1]✉, Renata Ďuračiová[3], Rastislav Jakuš[1]

Pivovar M., Mezei P., Ďuračiová R., Jakuš R., 2025. Sentinel-2 and environmental data as predictors of the spatiotemporal dynamics of bark beetle (Coleoptera: Scolytinae) - induced tree mortality in natural spruce forests. Ann. For. Res. 68(1): 137-154.

Abstract Biotic and abiotic disturbances affect forest ecosystems. Unlike sudden disturbances, bark beetle outbreaks are a gradual process. Bark beetle outbreak triggered by windstorm in Norway spruce (*Picea abies*) forests was analysed over a 6-year period (2016-2021) in mountainous conditions (890-2,100 m a.s.l.) with deep valleys and high ridges. The disturbance extent and dynamics were assessed via remote sensing (Sentinel-2 imagery) using a supervised maximum likelihood classification. Topographical variables, bark beetle-related spatial metrics and spectral indices were assessed for predictor importance for their influence on bark beetle-caused disturbance dynamics by boosted regression trees. The overall accuracy of the classification ranged from 87-92% (Kappa 0.84-0.89). Bark beetle spots were initiated mainly at relatively high altitudes and preferentially on exposed terrain. Spectral indices, such as the red-edge normalized difference vegetation index (RENDVI), played a consistent role across various years in predicting spot initiation. With respect to the spread of bark beetle spots, distance emerged as the most influential predictor across all years. Additionally, elevation and RENDVI had notable impacts on spot spreading. In the case of bark beetle spot initialization, the importance of different factors varied among years whereas for spot spreading distance was the most influential for each year.

Keywords: Sentinel-2, bark beetle, disturbances, *Ips typographus*, Norway spruce, *Picea abies*.

Addresses: [1]Institute of Forest Ecology Slovak Academy of Sciences (SAS), Zvolen, Slovak Republic. | [2]Technical University in Zvolen, Faculty of Ecology and Environmental Sciences, Zvolen, Slovak Republic. | [3]Slovak University of Technology in Bratislava, Faculty of Civil Engineering, Bratislava, Slovak Republic.

✉ **Corresponding Author:** Pavel Mezei (mezei@ife.sk).

Manuscript: received February 7, 2025; revised June 27, 2025; accepted June 29, 2025.

Introduction

In recent decades, the frequency and severity of wind-driven disturbances have increased in European coniferous forests, particularly affecting Norway spruce (*Picea abies* L. Karst.) populations (Nilsson & Nilsson 2004, Seidl et al. 2011, Senf & Seidl 2020). Wind disturbances and drought conditions have led to a substantial rise in the population of the Eurasian spruce bark beetle (*Ips typographus* L.), the primary infesting agents of Norway spruce (Økland & Berryman 2004, Wermelinger 2004, Marini et al. 2013, Økland et al. 2016) and its associated bark beetle species like *Pityogenes chalcographus* (L.) (Jakuš 1995). The proliferation of beetles in warmer and drier

climates has been a key factor in the doubling of canopy mortality in Central European temperate forests over the past 30 years (Schelhaas et al. 2003, Seidl et al. 2011, Senf & Seidl 2018).

Forests are naturally shaped by disturbances such as windthrows, which are often followed by bark beetle outbreaks - a pattern typical of Central European spruce forests (Parobeková et al. 2016, Holeksa et al. 2017). Such disturbances occur every two to three decades, usually requiring warm, dry conditions for bark beetle outbreaks (Mezei et al. 2017, Negrón and Cain, 2019, Lindman et al. 2023). Norway spruce, which accounts for a quarter of Europe's growing stock, has recently experienced unprecedented mortality rates due to the combined effects of drought, windthrow, and bark beetle outbreaks (Senf & Seidl, 2020, 2018, Hlásny et al. 2021).

Previous studies have utilized remote sensing data, such as Landsat (Hais & Kučera 2008, Havašová et al. 2015) and Sentinel-2 (Abdullah et al. 2019, Bárta et al. 2021, Huo et al. 2021) for mapping bark beetle infestations. While these approaches have proven valuable, effective forest management requires not only the detection of infestations but also the proactive identification of at-risk forest stands and the forecasting of future bark beetle outbreaks.

Predictive models for bark beetle infestations often rely on a variety of predictors, including forest structure, environmental variables, and bark beetle-specific spatial characteristics and distance functions (Ďuračiová et al. 2020, Fernández-Carrillo et al. 2024). Topographic-related data, such as potential solar radiation, are readily accessible and have demonstrated significant value in improving the predictive accuracy of bark beetle attack or bark beetle caused tree mortality models (Mezei et al. 2019). Bark beetle attacks exhibit spatial autocorrelation (Kamińska 2022) characterized by distinct phases of infestation initiation and spread (Coulson et al. 1989, Jakuš et al. 2003). Bark beetles typically infest trees near previous bark beetle infestations or areas affected by wind damage (Wichmann & Ravn 2001, Stadelmann et al. 2014, Potterf et al. 2019).

Incorporating spatial dynamics further enhances the predictive performance of such models. A critical input for many existing bark beetle forecasting models is terrestrial data obtained from forest inventories (Ďuračiová et al. 2020). Unfortunately, such data are often not publicly accessible, exhibit coarse spatial resolution (covering several hectares), and are updated only at intervals of approximately 10 years. These limitations reduce the timeliness and accuracy of predictions, highlighting the need for alternative data sources that can provide higher resolution and more frequent updates, such as remote sensing-based predictors. To address these shortcomings, models incorporating predictors derived predominantly from remote sensing data may offer greater accuracy and timeliness.

Remote sensing techniques can provide high-resolution, regularly updated datasets, which are crucial for improving the prediction and management of bark beetle infestations in dynamic forest environments. Remotely sensed data can also be used to extract important biophysical information on forests (trees) via vegetation indices, which are linked to various leaf physiological properties that affect satellite-observed spectral reflectance. Thus, a combination of certain bands extracted from digital remote sensing data can be used as surrogates for leaf (tree) or canopy (forest stand) biophysical properties (Jensen 2015), forest age (Chen et al. 2024) and other forest stand structural characteristics (Astola et al. 2019).

Huo et al. (2021) and Trubin et al. (2023, 2024) have shown that spectral indices derived from satellite data can be used for the identification of trees or parts of forest stands predisposed to bark beetle infestations. Ďuračiová et al. (2020) have used NDVI as one predictor of bark beetle-caused tree mortality. The influence of various predictors varies across different phases of bark beetle outbreaks and over time since the onset of an outbreak (Mezei et al. 2014, Ďuračiová et al. 2020).

The aim of our study was to identify appropriate predictive variables for forecasting bark beetle infestations in mountainous regions using available environmental and remote sensing data.

For this purpose, we i) mapped the spatiotemporal dynamics of bark beetle-induced tree mortality via Sentinel-2 images and ii) identified the role of topographic variables, bark beetle-related spatial metrics and spectral indices in bark beetle spot initialization and spreading. We focused on mountainous forests in a national park, where bark beetle-caused mortality has been mostly unaffected by human interventions in the past decades.

To address the spatiotemporal dynamics of tree mortality, analyses were conducted separately for each year, as well as for the processes of bark beetle spot initiation and spot expansion. Our study area is relatively small but consists of homogeneous forests with a concentrated wind-damaged zone.

Based on these objectives, we formulated the following hypotheses. The null hypothesis (H0) states that there is no difference in the relative feature importance of topographic and bark beetle-related spatial variables and spectral indices between the initialization and spreading of bark beetle infestation. H0: $FI_1 = FI_2$, where FI_1 and FI_2 represent the relative feature importance value of the several topographic variables, spectral indices and insect-related spatial metrics for the initialization and spreading, respectively. In contrast, the alternative hypothesis (HA) posits that the relative feature importance of these variables differs between the infestation initialization and spreading. HA: $FI_1 \neq FI_2$. To test these hypotheses, we aimed to assess the predictive importance of these variables for the initialization and spreading of the observed spatiotemporal dynamics of bark beetle-induced tree mortality.

Materials and Methods

Study area

The study area of the Suchá dolina valley in Slovakia (Fig. 1) is located in the High Tatra Mountains, belonging to the TANAP (Tatra National Park) region, with an area of more than 4,000 ha. The composition of stands consists of natural homogeneous populations of Norway spruce and, at higher elevations, dwarf pine (*Pinus mugo* Turra). The altitude ranges from 890 to 2,100 m a.s.l. The climate is characterized by low temperatures (annual average of 5.8°C) and moderate rainfall (750 mm per year) (Lapin et al. 2002).

In May 2014, the area was affected by the storm Žofia, which caused windthrow damage in an area of more than 400 ha. Since 2016, bark beetle infestations have started to occur on living trees in this area. The location and extent of the intervention and nonintervention zones for both landscapes were obtained from Havašová et al. (2017), with the study area marked in Fig. 1.

Figure 1 Map of the study area (Region of ineterest) located in the High Tatra National Park.

Study design

The design of the study was divided into three parts (Fig. 2): i) data collection and processing, ii) image classification and accuracy determination, and iii) analysis of predictor influence for bark beetle spot initiation and spread. In the first part, the Sentinel-2 satellite images were cropped for our study area. We further classified the images via region of interest (ROI) training sets of selected image classes and supervised the maximum likelihood classification (MAXL) algorithm with the semiautomatic classification plugin (SCP) (Congedo 2021). We reduced the number of classes by removing the non-forested areas (rock formations etc.). In the second part, we subjected the classification to statistical analyses to evaluate the overall classification accuracy (CA) of the classifications and their classes on an image-by-image basis. Next, we

created rasters with 9 topographic variables, 2 bark beetle-related spatial features (Table 2) and 5 spectral indices (Table 3). Finally, we analyzed the predictors of bark beetle spot initialization and spot spreading for each year via the boosted regression trees (BRT) (Elith et al. 2008).

Data collection and processing

We used freely available Sentinel-2 multispectral (MS) images (product Level-2A - Bottom of Atmosphere (BOA); tile numbers T34UCV and T34UDV; Copernicus Open Access Hub). Seven images were selected (Supplementary material) in the autumn aspect (Law & Nichol 2004) for the study period from 2015 – 2021, with no or very limited cloud cover (less than 10%). All bands with spatial resolutions of 10 and 20 m (Sentinel-2 bands: 2, 3, 4, 5, 6, 7, 8, 8a, 11, and 12) (Grabska et al. 2019) were used to increase spectral separation between beetle-infested and healthy trees (Wulder et al. 2006). The satellite data were projected into the coordinate system WGS 1984 UTM Zone 34 N (EPSG: 32634), and a part of Tatra National Park, specifically the Suchá dolina valley was delineated as the study area. All images were imported into a geographic information system (QGIS Development Team, 2024).

In our study, we adhered to rule of sufficient representativeness of image elements in the study area, i.e., that the minimum number of image features (pixels) in the training sets should be 10-100 times the number of channels required to produce a classification (Lillesand et al. 2015). In our case, for each class, we ensured that at least 280 times the number of pixels were present for a total of 10 channels. Additionally, we ensured that the ROI selection was uniformly distributed across the entire area, i.e., maximizing the variance of the ROIs. Fragments of classes with high variability in values were partitioned during ROI classification using the quantitative ROI selection method. All classes contained in their own ROIs for the 2021 model snapshot can be seen in Table 1. The classes prepared for classification were determined based on the type of forest damage and the tree species. Specific land cover types of non-vegetative origin were noted and later removed from the analysis. The classes were categorized as follows: Bark beetle caused tree mortality (BB; shadow and light), Windthrow area (Žofia storm in 2014; shadow and light), Healthy Spruce Forest (shadow and light), Dwarf Pine Forest (shadow and light), other and logging (before beetle detection in 2015).

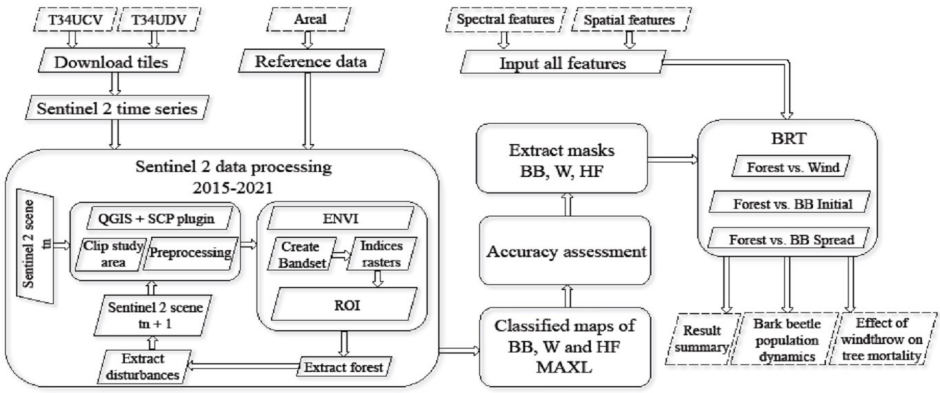

Figure 2 Study design. Abbreviations: T34UCV – tile identifier in the UTM map projection, specifying a precise geographic area within Zone 34U and tile CV; T34UDV – tile identifier in the UTM, specifying a precise geographic area within Zone 34U and tile DV; SCP – semiautomatic classification plugin; ROI – region of interest; MAXL – maximum likelihood classification; ENVI – environment for visualizing images software; BB – bark beetle-caused tree mortality; W – windthrow; HF – health spruce forest; BRT – boosted regression trees model; initial (initialization) and spreading (spreading).

Table 1 All classes stand mapped in this study with the number of polygons and pixels used as training for classification (based on multi-spectral image from 2021).

Classes	No. of polygons	No. of pixels
BB* shadow	10	307
BB* light	18	643
Wind shadow	4	452
Wind light	13	1 824
Forest shadow	14	2 127
Forest light	13	2 507
Dwarf Pine shadow	4	1 765
Dwarf Pine light	16	4 398
Other	22	13 219
Logging	4	900
Total	118	28 142

Note: *Bark beetle infestations

To facilitate post-classification analysis, we merged shaded and unshaded versions of each land cover class into unified categories (e.g., BB shadow and BB light into BB), as depicted in Fig. 5. This step reduced the class fragmentation caused by topographic shading and ensured consistent input for accuracy assessment and subsequent modeling. We categorized bark beetle-induced tree mortality (BB) into two groups: the initialization of bark beetle infestations refers to the initial emergence of new bark beetle spots causing tree mortality from all sites surrounded by healthy forests or other classes, while the spread of bark beetle infestations refers to the spread of tree mortality from previous BBs at time t_{n-1} or from windthrow (Jakuš et al. 2003, Ďuračiová et al. 2020). Any bark beetle-caused tree mortality more than 50 m away from previous bark beetle infestations was classified as "Initial".

Classification accuracy

To assess the accuracy of the classification results, we computed confusion matrices using photo-interpretation from the ROI, which were selected from all delineated ROIs based on high-resolution Google Earth imagery (from 2014). This resulted in the determination of CA and the kappa coefficient (Olofsson et al. 2013). Additionally, we computed the macro average F1 score (see Supplementary material), which is the harmonized average of producer and user accuracies (Zhong et al. 2019). For the overall accuracies, 95% confidence intervals were calculated based on the total variance of the accuracies (Olofsson et al. 2014). To assess the classification accuracy (CA), we used stratified random sampling on the 118 clean sub-areas described in Table 1, with the number of samples varying from year to year to maintain the rule of thumb of sufficient representativeness of image features (Lillesand et al. 2015). We followed the recommendation of Olofsson et al. (2014), we did not perform proportional allocation and increased the sample size for rarer classes.

Influence of predictor variables

We surveyed healthy forests and windthrows on the 2015 satellite image, and in subsequent years, we focused only on the bark beetle that caused tree mortality. The supervised classification was performed using the maximum likelihood algorithm (MAXL) implemented in the Semi-Automatic Classification Plugin (SCP) in QGIS. The resulting classified rasters were then used for calculating spectral vegetation indices for each year of the study. Based on previous studies (Baier et al. 2007, Mezei et al. 2019), the patterns of bark beetle-induced tree mortality are closely related to potential solar radiation and other abiotic characteristics that can be derived from digital terrain models. Since 2017, the Geodesy, Cartography and Cadastre Authority of the Slovak Republic has provided a digital terrain model (DTM), DTM 5.0, of the entire territory of the Slovak Republic, created from light detection and ranging (LiDAR) data (GCCA SR 2024). In our area of study, the density is 30 points per m^2 (Ďuračiová & Pružinec 2022).

The model is provided in raster format at a spatial resolution of 1 m and provides a suitable basis for modeling relief parameters and

potential solar radiation. To derive topographic characteristics, we used a digital elevation model (DEM) to calculate topographical position indices (TPIs), aspect, heat load indices (HLIs), and potential solar radiation. To calculate distances from bark beetle-induced tree mortality, we transformed all obtained classifications into vector files. We then took the vectors of the healthy forest and both classes of bark beetle-caused tree mortality from the 2016 image and applied them to the rasters from the set of vegetation indices, topography and bark beetle-derived spatial characteristics (Tables 2 and 3). Vegetation indices from one year prior to tree mortality detection were used as predictors.

We exported the data for each year into a single matrix and applied boosted regression trees - BRT (Elith et al. 2008), to assess the predictive influence on the initialization and spread of bark beetle-induced tree mortality. The response variables included the presence of spot initialization and the presence of spot spreading. We used explanatory variables described in Table 2 and 3. The BRT method is suitable for interpreting numerous independent characteristics relative to dependent parameters (Elith et al. 2008).

Our study involved testing forest mortality values in the current year against healthy forest indices from the previous year (t_{n-1}). Each BRT analysis for each year fitted a function minimizing the error between the actual and predicted values. Boosted regression trees utilize multiple decision tree predictions to make a final prediction which is achieved by the boosting process, where each tree is constructed on the basis of the errors of the preceding tree, progressively increasing the model's efficiency (XGBoost, 2024). Regression trees with over 5,000 iterations were constructed,

Table 2 List of topographic and bark beetle-related spatial variables used in the BRT analyses.

Topographic variables	Short description	Source	Abbreviation
Elevation	Elevation above sea level (from a DEM).	GCCA SR 2024	Elevation
Heat load index	Normalized angle of incident solar radiation calculated from the DEM.	McCune & Keon 2002	HLI
Slope	The incline of a surface, measured in degrees from horizontal (0°-90°).	ESRI 2024	Slope
Solar radiation	Potential solar radiation calculated on the basis of the DEM.	Ďuračiová & Pružinec 2022	Solar radiation
Aspect transformed to angular distance from the south*	The slope azimuth calculated from the DEM transformed into the angular distance from the south (‘southness’) measured in degrees (0°-180°).	Deng et al. 2009	Aspect
Topographic position index 50	Differences of each cell value of DEM and the mean elevation of the specified neighborhood of that cell (50 m, 100 m, 250 m, 500 m).	Weiss 2001; Ďuračiová & Pružinec 2022	TPI 50
Topographic position index 100			TPI 100
Topographic position index 250			TPI 250
Topographic position index 500			TPI 500
Bark beetle-related spatial variables	**Short description**	**Source**	**Abbreviation**
Distance	Distance from bark beetle outbreaks.	Jakuš et al. 2005; Ďuračiová et al. 2020	Distance
Pressure Initial	Amount of infested forest around a cell. They are inverted and normalized using the maximum initialization and spreading distance from the first year of analysis.	Kärvemo et al. 2014a	Pressure Initial
Pressure Spread			Pressure Spread

Note: *Aspect is an important terrain parameter, but it is difficult to include it directly in the analysis because of its angular scale (0° to 360°, with values of 0° and 360° being close to each other).

Table 3 List of spectral indices used in the BRT analyses.

Variables	Short description	Source	Abbreviation
Enhanced vegetation index	It uses the blue reflectance region to correct for soil background signals and to reduce atmospheric influences, including aerosol scattering.	Huete et al., 2002	EVI
Leaf area index	This index is used to estimate foliage cover and to forecast crop growth and yield.	Baret & Guyot, 1991	LAI
Normalized difference vegetation index	This index is a measure of healthy, green vegetation use of the highest absorption and reflectance regions of chlorophyll.	Rouse et al., 1974	NDVI
Plant senescence reflectance index	This index maximizes the sensitivity of the index to the ratio of bulk carotenoids to chlorophyll. An increase in PSRI indicates increased canopy stress (carotenoid pigment), the onset of canopy senescence, and plant fruit ripening.	Merzlyak et al., 1999	PSRI
Red-Edge NDVI	This index is a modification of the traditional broadband NDVI. It capitalizes on the sensitivity of the vegetation red edge to small changes in canopy foliage content, gap fraction, and senescence.	Gitelson & Merzlyak, 1994	RENDVI
Simple ratio index	Ratio of the wavelength with highest reflectance for vegetation and the wavelength of the deepest chlorophyll absorption.	Birth & McVey, 1968	SRI

ensuring the inclusion of rare classes such as BB initialization. Visualization of fitted functions in the BRT model is achieved via partial dependence plots, accounting for the effect of all other variables (Elith et al. 2008). This approach predisposes BRT models to capture nonlinear relationships between input variables and the target variable. Model evaluation relies on the area under the curve (AUC), with higher values indicating better-fitting models (Parisien and Moritz 2009).

We used a Bernoulli family algorithm to model the fit, mapping values of 0 and 1 (presence of bark beetle-initialization or spreading pixels). All the models were generated in R 4.1.3 (R Core Team, 2020) via the gbm package (Ridgeway 2024) and extensions developed by Elith et al. (2008) and Leathwick et al. (2011).

Results

Time series analysis of beetle-caused tree mortality

Windthrown areas acted as sources of bark beetle-induced tree mortality in the surrounding forest. The Žofia windstorm and bark beetles affected a total of 1,253 hectares, with 401 hectares and 852 hectares attributed to each, respectively. Between 2015 and 2017, during the initial and epidemic phases, 804.5 hectares of forest died, with 401 hectares due to windthrow and 403.5 hectares due to bark beetles. The area of dead trees in the post-epidemic phase (2018-2021) was 449 ha (bark beetle-caused forest damage only), as shown in Fig. 3. Tree mortality caused by bark beetles exhibited a negative trend until 2019, after which it increased. Notably, the 2018 and 2019 image classifications revealed an increase in the area of healthy forest. This was probably caused by forest succession in areas previously affected by wind and bark beetles.

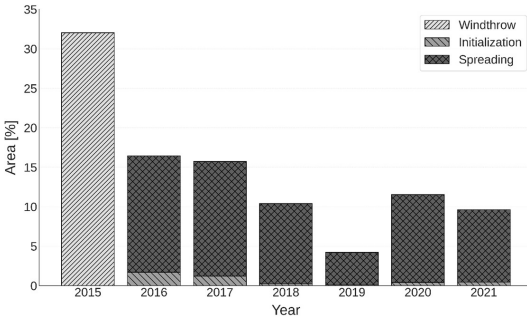

Figure 3 Temporal dynamics of relative tree mortality driven by windthrow and bark beetle infestations in 2015 – 2021.

Classification accuracy of Sentinel-2 data

The evaluation of the overall classification accuracy and the influence of random factors that may have caused misclassification (forest, wind, bark beetle) are shown in Table 4. The CA was approximately 92% ($p < 0.01$). The influence of the random component is interpreted by the kappa index, whose mean value is 0.88. The influence of the random factors was statistically insignificant. Owing to the separated classification of the unshaded and shaded parts, we achieved greater variability in the average classification accuracy of each class, which has a positive effect on increasing the accuracy of the overall image classification.

Table 4 Overall classification accuracy (CA) considering a random component via the kappa index and p-value.

Year	CA* [%]	Kappa	Δp
2015	90.87	0.89	± 0.0029
2016	89.45	0.87	± 0.0032
2017	90.68	0.88	± 0.0032
2018	91.15	0.89	± 0.0032
2019	91.56	0.89	± 0.0031
2020	87.39	0.84	± 0.0039
2021	91.81	0.89	± 0.0032

The classification visualization based on the Sentinel-2 multispectral images in Fig. 4 clearly interprets the sensitivity of the unshaded and shaded portions of the healthy and damaged forest. Figure 4 shows the classification result of the image from 2015, prior to beetle caused tree mortality (Fig. 5).

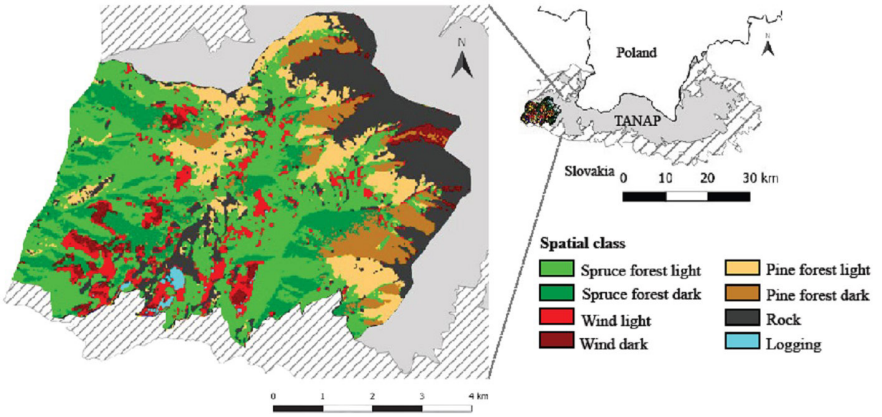

Figure 4 MAXL classification result for the 2015 image of the Suchá dolina Valley.

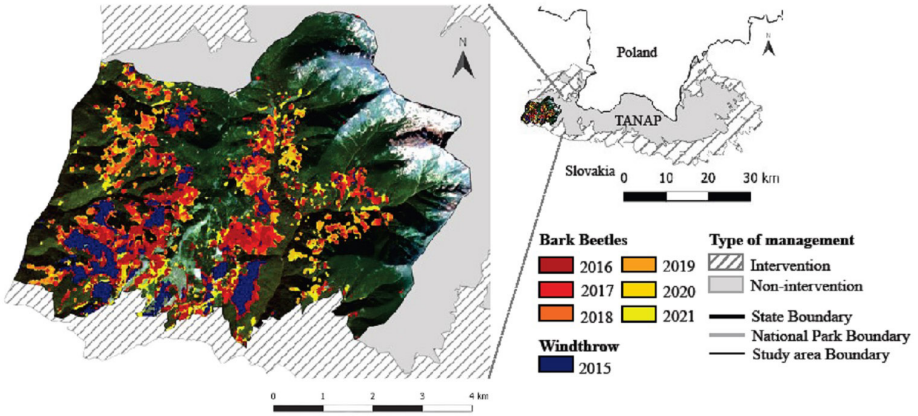

Figure 5 Spatial distribution of bark beetle-induced tree mortality time series from 2016 – 2021 and the windthrow area recorded in 2015.

Effects of predictor variables

BRTs were used for the analysis of the effects of predictor variables on tree mortality caused by bark beetles. The importance of the topographic variables, bark beetle-related spatial variables and spectral indices is listed in Table 5. To interpret the effect of predictor variables on bark beetle spot initialization and spread in each year, we selected the 4 characteristics that had the strongest variable importance according to the BRT model. The shape of the relationship with the initialization or spread of beetle-caused tree mortality is in Figs. 6 and 7. Partial dependence values show the effect of a variable on the response variable after accounting for the average effects of all other variables in the model (Friedman 2001, Friedman & Meulman 2003). The vertical axis of all the graphs shows the fitted BRT function. If the fitted function is > 0, the probability that a given pixel experienced tree mortality by bark beetles is above 50%.

Initialization of the bark beetle caused tree mortality

In 2016, the first year of tree mortality, topographic and bark beetle-related spatial metrics were more impactful than spectral indices (Fig. 6a-d). Distance had a predictive importance ranging from 9.9% to nearly 24%, indicating that bark beetles are over 50% likely to infest forests located 50 to cca 400 meters from the stand edge. More than 90% of infested pixels fell within this distance range (Fig. 6a). Other variables had less than 8% importance (Table 5).

Table 5 Importance of topographic variables, bark beetle-related spatial metrics and spectral indices across all forest damage classes from 2016-2021 based on BRT analysis. Variables with an influence above 10% are highlighted by bold font. For a description of the predictor variables, we refer to Tables 2 and 3.

Variable		2016		2017		2018		2019		2020		2021	
		Initial	Spread	Initial	Spread	Initial	Spread	Initial	Spread	Initial	Spread	Initial	Spread
BB sp.m.	Distance	**11.9**	**19.6**	**20.2**	**19.2**	**13.7**	**12.1**	**9.9**	**22.7**	**23.7**	**21.7**	**25.6**	**17.3**
	BB presure	7.2	**17.5**	6.9	5.7	5.3	7.6	3.5	8.1	5.9	8.5	3.1	5.6
Spatial	Elevation	8.8	7	6.7	8.6	3.4	**11**	7.6	**10**	8.1	9.7	4.7	8.5
	Slope	5.4	4.1	4	4.7	1.6	5.8	2.5	3.5	3	3.7	1.6	4.6
	Aspect	4.9	3	4	4.1	1	3.5	**12.8**	2.4	4	3.1	1.4	4.7
	TPI_500	7.1	4.2	5	4	7	4.7	1.4	2.9	**11.5**	2.9	2.7	3.6
	TPI_250	5.1	3.1	4.2	3.9	1.1	4.5	3.7	2.7	8	2.5	3.9	3
	TPI_100	5	2.8	4.1	4.2	1.6	4.7	6.3	2.7	4.5	2.8	2.2	2.9
	TPI_50	5.6	3.4	3.9	4	1.5	4.4	1.9	2.7	3.4	2.9	1.1	3.7
	Solar radiation	5.1	2.9	4.9	3.5	3.1	3.8	4.7	2.4	2.4	3	2.2	3.3
	HLI	4.1	2.5	3.9	3.2	1.2	3	3.1	1.8	4.1	3	1.9	3.9
Spectral	NDVI	5	4.5	8.1	7.8	9.1	7.6	8.3	7.9	3	7.2	2.6	5.4
	PSRI	6.9	7	4.7	6.1	**23.5**	5.6	3.6	4.6	6.3	8.6	5.4	**15.5**
	EVI	6.4	4.7	4.8	5.3	2	6.2	**12.8**	5.1	3	4.7	**36.1**	7.9
	SRI	4.7	4.3	8	8.7	**10**	7.6	8.6	**10.7**	3	6.4	4	4.6
	RENDVI	6.8	9.4	6.6	7	**14.9**	7.9	9.3	**10**	6	9.3	1.4	5.5
Training data AUC		0.99	0.976	0.99	0.981	0.998	0.98	0.999	0.994	1	0.98	1	0.992
CV cor*		0.81	0.75	0.9	0.74	0.93	0.73	0.9	0.85	0.94	0.78	0.97	0.8

Note: BB sp.m.: Bark beetle related spatial metrics; Spatial: spatial characteristics; Spectral: Spectral characteristics; BB pressure: Bark beetle pressure; CV cor*: CV correlation*; Cross-validation correlation in BRT; With the PSRI and RENDVI showing opposite effects, higher PSRI values correlated with greater infestation initiation, and vice versa; While PSRI and RENDVI had weak predictive values.

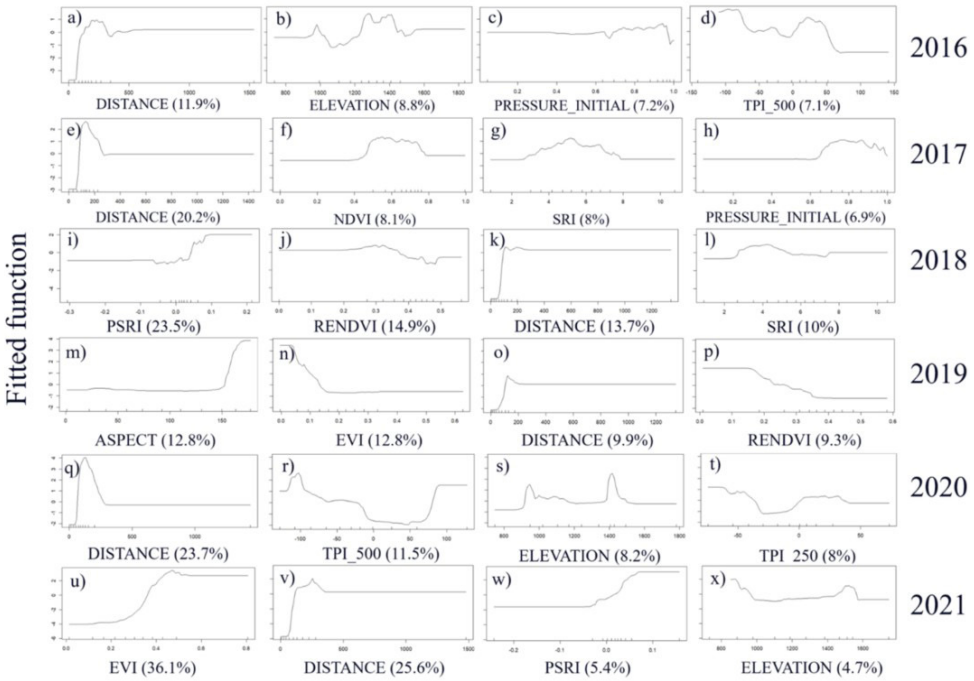

Figure 6 Most important predictor variables for initial bark beetle cased tree mortality based on BRT analysis between 2016 – 2021.

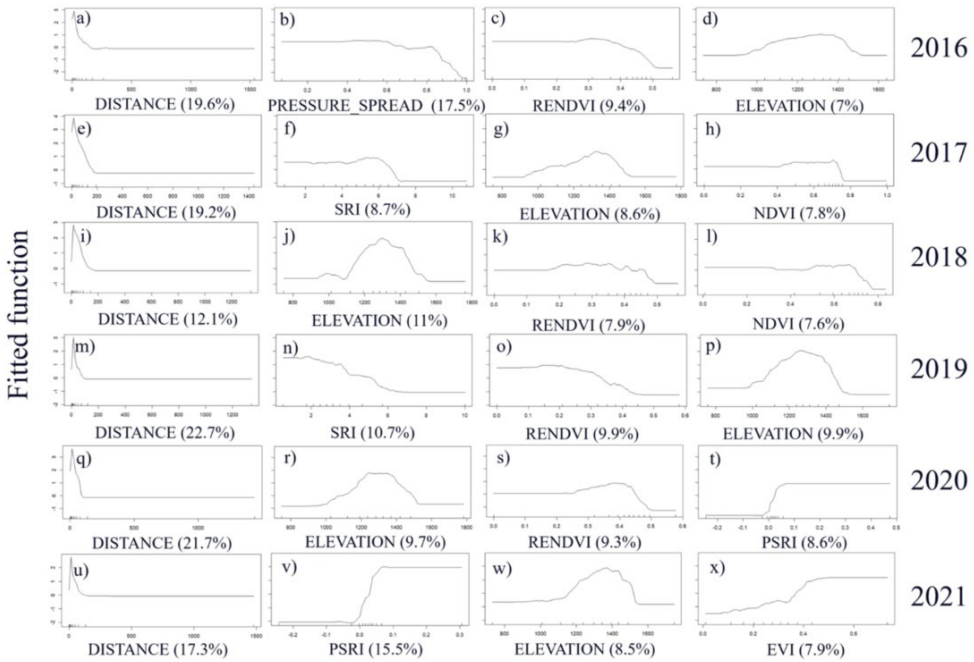

Figure 7 Most important predictor variables for the spread of bark beetle-induced tree mortality based on BRT analysis in the Suchá dolina Valley between 2016 – 2021.

In the second year of the outbreak (2017) (Fig. 6e-h), the importance of distance increased to over 20%. Infested pixels were again concentrated within 100–300 meters of windthrown plots (Fig. 6e). NDVI analysis revealed that pixels most susceptible to beetle initialization had NDVI values between 0.5 and 0.7, with similar predictive importance as SRI.

For newly infested pixels in 2018 (Fig. 6i-l), the PSRI emerged as the most important variable with a significance of 23.5%, followed by RENDVI at 14.9%. Distance patterns remained consistent with previous years, showing initialization at PSRI values of 0.05-0.2 and RENDVI values below 0.3 at distances of 100 – 150 meters from the stand edge.

In 2019 (Fig. 6m-p), the initial disturbance resulted in the smallest area of infestation, with under 120 pixels recorded (Table 1). Distance showed a predictive importance of nearly 10%. The aspect also played a role, suggesting that bark beetles favored northern slopes.

By 2020 (Fig. 6q-t), distance had a predictive importance of almost 24%, correlating strongly with over 90% of infested pixels located between 50 and 250 meters from the stand edge. TPI_500 showed nearly 12% importance, indicating susceptibility at altitudes above 900 m a.s.l., while PSRI and RENDVI had weak perspective values (Table 5).

In the final year analyzed (2021) (Fig. 6u-x), EVI and distance were key factors in new bark beetle disturbances, with variable importance values of 36% and 26%, respectively. New infestations occurred at EVI values between 0.4 and 0.8 and distances of 100 to 300 meters from the stand edge.

Spread of bark beetle-caused tree mortality

In 2016, distance was the most important factor influencing bark beetle spread, with a variable importance of nearly 20%. The highest probability of spread occurred at distances to 180 meters from existing infestations. Additionally, the pressure from beetle outbreaks was significant, with an importance of 17.5%. Most infestations were found at elevations ranging from 1,100 to 1,500 meters (Fig. 7a-d).

The following year, distance continued to dominate as a predictor, showing an importance of 19%. However, the second most important variable shifted to SRI, with spread occurring at index values of 1-7 (Fig. 7e-h).

In the next assessment (2018), distance remained a strong predictor with an importance of 12%. The patterns observed were similar to those in previous years, with spread occurring at distances to 150 meters. Elevation also played a significant role, achieving an importance of 11% (Fig. 7i-l).

As bark beetle activity declined, distance still proved crucial, showing an importance of almost 23%. Most infestations occurred within 100 meters from the stand edge. Notably, the SRI gained significance, with a predictive importance of nearly 11% at levels 0 to 4. RENDVI and elevation both had around 9.9% importance (Fig. 7m-p).

In the following year (2020), distance continued to be the primary predictor for bark beetle spread with an importance of 22%. Elevation followed as the second most significant factor at nearly 10%. RENDVI showed over 9% predictive ability at the index levels from 0.3 to 0.45 (Fig. 7q-t).

In the final year of the study, distance remained critical with over 17% importance and similar patterns to those observed previously.

The PSRI increased to a variable importance of 15.5%, indicating that higher PSRI values correlated with beetle spread. Elevation maintained an importance of about 8.5%. EVI, pressure spread, and RENDVI all had variable importance values below 8%, with EVI showing a positive trend for beetle spread while pressure spread and RENDVI exhibited negative trends (Fig.7, Table 5).

Discussion

During the period of 2016-2021, approximately 1,200 ha of forest were affected by wind (401 ha) and bark beetles (852 ha) disturbances in the 4,000-ha study area, as noted from Sentinel-2 images. Boosted regression trees have been applied to identify predictors of bark beetle-induced tree mortality. In the case of

bark beetle spot initialization, the importance of different factors varied among years (Table 5, Fig. 6). For spot dispersal, distance was the most important factor every year (Table 5 and Fig. 7). These findings are in agreement with those of previous works (Wichmann & Ravn 2001, Lausch et al. 2011, Potterf et al. 2019, Stadelmann et al. 2014, Ďuračiová et al. 2020, Fernández-Carrillo et al. 2024).

Quality of Satellite Data Classification

Compared with Lausch et al. (2013), who achieved a classification accuracy of 64% for infested and healthy trees, the methods applied in our study achieved a significantly higher overall classification accuracy, averaging approximately 90% over the years 2015-2021. This improvement is corroborated by the kappa index, which has a mean value of 0.88, indicating strong agreement beyond chance. In addition, the statistical analysis revealed that the influence of random factors such as forest conditions, wind and bark beetle infestations was insignificant, further confirming the robustness of our classification approach.

Factors related to bark beetle spot initialization

The bark beetle outbreak was initiated by a windstorm in May 2014. The most important variable influencing tree mortality is often the number of colonized wind-felled trees (Kärvemo et al. 2014b), which, in our case, could be stronger than the effect of topography. The most important predictors of windstorms are usually severe weather conditions and the height of *P. abies* (Kärvemo et al. 2023). However, the occurrence of such events is very infrequent, especially for a timeframe, as represented in our study. *Ips typographus* developed on freshly broken and uprooted spruce trees (Hroššo et al. 2020). The most influential predictors of the initialization of new spots were distance, bark beetle population pressure, altitude, topographic position and spectral indices (RENDVI, PSRI).

Bark beetle population-related spatial features, particularly the distance from previous infestation edges, emerged as significant predictors. Infestations were concentrated within 50 – 300 m from previous infestation edges. We only consider an infestation to be a new spot initialization if it is more than 50 m from the previous infestation. The 50 m distance threshold is the result of our methodology and the data used. The predictive importance of distance was each year ranked as the most important factor for bark beetle spread. These findings are in agreement with the results of Wichmann and Ravn (2001), Stadelmann et al. (2014), Potterf et al. (2019) and Fernández-Carrillo et al. (2024). Another important variable was bark beetle population pressure. This was an important factor at the beginning of the bark beetle outbreak (Kärvemo et al. 2014b).

In our study area, the wind-damaged stands were located at relatively low elevations, and bark beetle infestations spread upward. The observed altitudinal spread of bark beetle infestations moving from lower to higher elevations may be closely linked to thermal conditions. Warmer temperatures at lower altitudes can accelerate insect development, increase the number of generations per season, and enhance fecundity, as demonstrated in several bark beetle species (Jönsson et al. 2009). This may lead to initial outbreaks at lower elevations, which subsequently expand to higher altitudes. While temperature and precipitation are key climatic drivers of bark beetle dynamics (Marini et al. 2012), these variables were not directly included in our analysis.

In mountainous regions, microclimatic variability can significantly influence insect life cycles, yet such fine-scale data are often unavailable or unreliable when derived from distant weather stations. To address this, we used solar radiation as a thermal proxy, as it can be modeled directly from DEM and reflects local topographic conditions (Mezei et al. 2019). Despite its limitations, this approach provides a spatially explicit estimate of thermal input, which may offer insights into bark beetle population dynamics across heterogeneous landscapes.

The topographic position index (TPI_500) was also an important variable. Stadelmann et

al. (2014) reported that terrain exposure is a strong predictor of wind damage and bark beetle infestation. Furthermore, topographical factors such as elevation influence the likelihood of infestation, with specific thresholds identified for susceptibility. Elevation and TPI_500 had some impact on the infestation of trees by bark beetles. The results show that the initialization of the outbreaks starts at lower altitudes than their spread. Other local topographical variables had weak effects on tree infestations (Table 5).

The spectral indices did not exhibit homogenous patterns during the study. The RENDVI was an important variable in almost all years. It is highly sensitive to variations in chlorophyll content, which can serve as reliable indicators of the early stages of leaf senescence. Furthermore, the events that occur in senescing and aging of leaves are similar to those occurring in plants under stress. It is also distinct under conditions with high chlorophyll concentrations or landscapes with high leaf area indices (Gitelson & Merzlyak 1994).

The RENDVI has shown proficiency in identifying not only significant damage to spruce stands but also subtle variations in tree physiological conditions, particularly in instances where high defoliation levels are not evident (Mišurec et al. 2016). Additionally, the RENDVI is correlated with nitrogen concentrations (de Oliveira et al. 2017), above-ground biomass (Imran et al. 2020), discoloration (Xie et al. 2018), and soil moisture (Siegfried et al. 2019). Additionally, environmental factors such as elevation, influenced the likelihood of infestation, with specific thresholds identified for susceptibility.

An important vegetation index for forest health assessment was the plant senescence reflectance index (PSRI), which measures needle senescence.

Factors related to bark beetle spot spreading

Despite fluctuations in bark beetle activity over time, distance remained consistently the most influential predictor of bark beetle spot spreading. The role of distance represents a key distinction between the processes of spot initialization and spot spreading. In the case of spot initialization, the importance of distance was observed to vary over time. In contrast, for spot spreading, distance was the most important predictor across all years. Analyses of bark beetle outbreaks suggest that the infestation process mainly occurs at a scale of a few hundred meters (Kautz et al. 2011, Kärvemo et al. 2014a, Potterf et al. 2019, Müller et al. 2022). In our case, distance was among the most common variables with high variable importance for bark beetle spot spread (Table 5). The spread occurred mainly at altitudes of 1,200 – 1,400 m. Other significant factors, which had a notable impact in all years, were elevation and RENDVI index. This vegetation index was also an important predictor of spot initialization.

Limitations of the study

The main limitation of our study is the relatively small study area and short time span; however, image processing with high-resolution satellite imagery can be time consuming, especially for highly diverse terrains where long mountain range spans complicate tree and disturbance identification. Other studies that used Sentinel-2 images used specific trees as basic sample sizes (Dalponte et al. 2023), polygons of different sizes (Lastovicka et al. 2020, Bárta et al. 2021), several hundred hectares of forests (Huo et al. 2021) or entire landscapes (Migas-Mazur et al. 2021).

While climate was not taken into account in this study, we included potential solar radiation as an explanatory variable linked to preferred infestation locations (Hroššo et al. 2020), and solar radiation acted as one of the influencing variables, at least during the peak phase of the outbreak (Mezei et al. 2014, Mezei et al. 2019).

The importance of solar radiation suggests that temperature stress is exacerbated by solar exposure and further implies a direct physiological influence of these variables on tree

health. Solar radiation was positively associated with bark beetle-caused tree mortality in 2 of the 4 surveyed locations in California (Young et al. 2023). Hence, in the present study, solar radiation was not among the most influential variables. Owing to the small size of the study area (4,000 ha), we did not expect large differences in bark beetle population dynamics (Lindman et al. 2023) among the different forest patches. The importance of variables can vary during drought periods (Müller et al. 2022, Nardi et al. 2023).

Practical implementation

In our study, we used only remote sensing data and a DEM, and we did not include data from forest management plans. The resolution of the forest management plan data is much lower than the satellite data we employed. However, tree dimensions and tree age are variables usually reported in forest management plans and are highly important predictors for bark beetle infestations (Ďuračiová et al. 2020). We used vegetation indices instead. Despite this limitation, we achieved relatively reliable results. This finding shows that models for predicting bark beetle infestations can be constructed on the basis of only remote sensing data. Models can be incorporated into online web services and used for bark beetle population control or incorporated into online decision support systems. Our results have the potential to significantly improve forest protection measures.

Conclusion

We have shown that models based on accessible environmental data and remote sensing information, especially vegetation indices, can effectively predict bark beetle infestations.

In the case of bark beetle spot initialization, the importance of different factors varied among years. Bark beetle spots were initiated mainly at middle altitudes and preferentially on exposed terrain. Spectral indices, particularly RENDVI, play a consistent role across various years in predicting spot initiation.

With respect to the spread of bark beetle spots, distance emerged as the most influential predictor in all years, underscoring its pivotal role in understanding infestation dynamics. Additionally, elevation and the RENDVI had notable impacts on spot spreading. Practical implications suggest that models based on freely accessible topographical and remote sensing data, can reliably predict bark beetle infestations.

Conflict of interest

The authors declare that they have no conflict of interest.

Acknowledgements

This research was supported by Horizon Europe (Grant ID 101078970), project RESDINET 'Network for novel remote sensing technologies in forest disturbance ecology', and the Slovak Research and Development Agency under Contract No. APVV-22-0151 and by grant VEGA 2/0155/22 and 1/0626/25 of the Scientific Grant Agency of the Ministry of Education, Science, Research, and Sport of the Slovak Republic and the Slovak Academy of Sciences. We also thank the two anonymous reviewers for their valuable comments and suggestions that improved the paper.

References

Abdullah H., Skidmore A.K., Darvishzadeh R., Heurich M., 2019. Sentinel-2 accurately maps green-attack stage of European spruce bark beetle (*Ips typographus*, L.) compared with Landsat-8. Remote Sensing in Ecology and Conservation 5(1): 87–106. https://doi.org/10.1002/rse2.93

Astola H., Häme T., Sirro L., Molinier M., Kilpi J., 2019. Comparison of Sentinel-2 and Landsat 8 imagery for forest variable prediction in boreal region. Remote Sensing of Environment 223: 257–273. https://doi.org/10.1016/j.rse.2019.01.019

Baier P., Pennerstorfer J., Schopf A., 2007. PHENIPS – A comprehensive phenology model of *Ips typographus* (L.) (Col., Scolytinae) as a tool for hazard rating of bark beetle infestation. Forest Ecology and Management 249(1–3): 171–186. https://doi.org/10.1016/j.foreco.2007.05.020

Baret F., Guyot G., 1991. Potentials and limits of vegetation indices for LAI and APAR assessment.

Remote Sensing of Environment 35(2): 161–173. https://doi.org/10.1016/0034-4257(91)90009-u

Bárta V., Lukeš P., Homolová L., 2021. Early detection of bark beetle infestation in Norway spruce forests of Central Europe using Sentinel-2. International Journal of Applied Earth Observation and Geoinformation 100: 102335. https://doi.org/10.1016/j.jag.2021.102335

Birth G., McVey G., 1968. Measuring the color of growing turf with a reflectance spectrophotometer. Agronomy Journal 60(4): 640–643. https://doi.org/10.2134/agronj1968.00021962006000060016x

Chen J., Du H., Mao F., Huang Z., Chen C., Hu M., Li X., 2024. Improving forest age prediction performance using ensemble learning algorithms based on satellite remote sensing data. Ecological Indicators 166: 112327. https://doi.org/10.1016/j.ecolind.2024.112327

Congedo L., 2021. Semi-Automatic Classification Plugin. Retrieved from https://semiautomaticclassificationmanual.readthedocs.io/_/downloads/en/latest/pdf/

Coulson R.N., Feldman R.M., Sharpe P.J.H., Pulley P.E., Wagner T.L., Payne T.L., 1989. An overview of the TAMBEETLE model of *Dendroctonus frontalis* population dynamics. Ecography 12(4): 445–450. https://doi.org/10.1111/j.1600-0587.1989.tb00921.x

Dalponte M., Cetto R., Marinelli D., Andreatta D., Salvadori C., Pirotti F., Frizzera L., Gianelle D., 2023. Spectral separability of bark beetle infestation stages: A single-tree time-series analysis using Planet imagery. Ecological Indicators 153: 110349. https://doi.org/10.1016/j.ecolind.2023.110349

de Oliveira L.F.R., de Oliveira M.L.R., Gomes F.S., Santana R.C., 2017. Estimating foliar nitrogen in Eucalyptus using vegetation indexes. Scientia Agricola 74(1): 142–147. https://doi.org/10.1590/1678-992x-2015-0477

Deng Y., Goodchild M.F., Chen X., 2009. Using NDVI to define thermal south in several mountainous landscapes of California. Computers & Geosciences 35(3): 327–336. https://doi.org/10.1016/j.cageo.2008.08.005

Ďuračiová R., Muňko M., Barka I., Koreň M., Resnerová K., Holuša J., Blaženec M., Potterf M., Jakuš R., 2020. A bark beetle infestation predictive model based on satellite data in the frame of decision support system TANABBO. iForest 13(2): 215–223. https://doi.org/10.3832/ifor3271-013

Ďuračiová R., Pružinec F., 2022. Effects of terrain parameters and spatial resolution of a digital elevation model on the calculation of potential solar radiation in the mountain environment: A case study of the Tatra Mountains. ISPRS International Journal of Geo-Information 11(7): 389. https://doi.org/10.3390/ijgi11070389

Fernández-Carrillo, Á., Franco-Nieto, A., Yagüe-Ballester, M.J. and Gómez-Giménez, M., 2024. Predictive Model for Bark Beetle Outbreaks in European Forests. Forests, 15(7), p.1114. https://doi.org/10.3390/f15071114

Elith J., Leathwick J.R., Hastie T., 2008. A working guide to boosted regression trees. Journal of Animal Ecology 77(4): 802–813. https://doi.org/10.1111/j.1365-2656.2008.01390.x

ESRI, 2024. ArcGIS Pro 3.0. Environmental Systems Research Institute, Redlands, CA.

ENVI 5.7, 2010. Exelis Visual Information Solutions.

Friedman J.H., 2001. The role of statistics in the data revolution? International Statistical Review 69(1): 5–10. https://doi.org/10.1111/j.1751-5823.2001.tb00474.x

Friedman J.H., Meulman J.J., 2003. Multiple additive regression trees with application in epidemiology. Statistics in Medicine 22(15): 1365–1381. https://doi.org/10.1002/sim.1501

GCCA SR, 2024. Airborne Laser Scanning and DTM 5.0.

Gitelson A., Merzlyak M.N., 1994. Quantitative estimation of chlorophyll-a using reflectance spectra: Experiments with autumn chestnut and maple leaves. Journal of Photochemistry and Photobiology B: Biology 22(2): 247–252. https://doi.org/10.1016/1011-1344(93)06963-4

Grabska E., Hostert P., Pflugmacher D., Ostapowicz K., 2019. Forest stand species mapping using the Sentinel-2 time series. Remote Sensing 11(10): 1197. https://doi.org/10.3390/rs11101197

Hais M., Kučera T., 2008. Surface temperature change of spruce forest as a result of bark beetle attack: Remote sensing and GIS approach. European Journal of Forest Research 127(3): 327–336. https://doi.org/10.1007/s10342-008-0208-8

Havašová M., Bucha T., Ferenčík J., Jakuš R., 2015. Applicability of a vegetation indices-based method to map bark beetle outbreaks in the High Tatra Mountains. Annals of Forest Research 58(2): 295–310. https://doi.org/10.15287/afr.2015.388

Havašová M., Ferenčík J., Jakuš R., 2017. Interactions between windthrow, bark beetles and forest management in the Tatra National Parks. Forest Ecology and Management 391: 349–361. https://doi.org/10.1016/j.foreco.2017.01.009

Hlásny T., Zimová S., Merganičová K., Štěpánek P., Modlinger R., Turčáni M., 2021. Devastating outbreak of bark beetles in the Czech Republic: Drivers, impacts, and management implications. Forest Ecology and Management 490: 119075. https://doi.org/10.1016/j.foreco.2021.119075

Holeksa J., Jaloviar P., Kucbel S., Saniga M., Svoboda M., Szewczyk J., Szwagrzyk J., Zielonka T., Żywiec M., 2017. Models of disturbance driven dynamics in the West Carpathian spruce forests. Forest Ecology and Management 388: 79–89. https://doi.org/10.1016/j.foreco.2016.08.026

Hroššo B., Mezei P., Potterf M., Majdák A., Blaženec M., Korolyova N., Jakuš R., 2020. Drivers of spruce bark beetle (*Ips typographus*) infestations on downed trees after severe windthrow. Forests 11(12): 121290. https://doi.org/10.3390/f11121290

Huete A., Didan K., Miura T., Rodriguez E.P., Gao X., Ferreira L.G., 2002. Overview of the radiometric and biophysical performance of the MODIS vegetation indices. Remote Sensing of Environment 83(1): 195–213. https://doi.org/10.1016/S0034-4257(02)00096-2

Huo L., Persson H.J., Lindberg E., 2021. Early detection

of forest stress from European spruce bark beetle attack, and a new vegetation index: Normalized distance red & SWIR (NDRS). Remote Sensing of Environment 255: 112240. https://doi.org/10.1016/j.rse.2020.112240

Imran A.B., Khan K., Ali N., Ahmad N., Ali A., Shah K., 2020. Narrow band based and broadband derived vegetation indices using Sentinel-2 imagery to estimate vegetation biomass. Global Journal of Environmental Science and Management 6(1): 97–108. https://doi.org/10.22034/gjesm.2020.01.08

Jakuš R., 1995. Bark beetle (Col., Scolytidae) communities and host and site factors on tree level in Norway spruce primeval natural forest. Journal of Applied Entomology, 119(1-5): 643-651. https://doi.org/10.1111/j.1439-0418.1995.tb01352.x

Jakuš R., Grodzki W., Jezik M., Jachym M., 2003. Definition of spatial patterns of bark beetle Ips typographus (L.) outbreak spreading in Tatra Mountains (Central Europe), using GIS. In: Ecology, Survey and Management of Forest Insects, 1–5 September 2002, PA, USA. US Dept of Agriculture, Forest Service, Northeastern Research Station, pp. 25–32.

Jakuš R., Ježík M., Kissiyar O., Blaženec M., 2005. Prognosis of bark beetle attack in TANABBO model. In: GIS and Databases in the Forest Protection in Central Europe, 27–35 November 2004, Krakow, Poland. pp. 35–43.

Jensen J.R., 2015. Introductory digital image processing: A remote sensing perspective. 4th ed. Pearson, Boston, 684 p.

Jönsson A.M., Appelberg G., Harding S., Bärring L., 2009. Spatio-temporal impact of climate change on the activity and voltinism of the spruce bark beetle, *Ips typographus*. Global Change Biology 15(4): 486–499. https://doi.org/10.1111/j.1365-2486.2008.01742.x

Kamińska A., 2022. Spatial autocorrelation based on remote sensing data in monitoring of Norway spruce dieback caused by the European spruce bark beetle Ips typographus L. in the Białowieża Forest. Sylwan 166(7): 572–582. https://doi.org/10.26202/sylwan.2022072

Kärvemo S., Van Boeckel T.P., Gilbert M., Grégoire J.-C., Schroeder M., 2014a. Large-scale risk mapping of an eruptive bark beetle – Importance of forest susceptibility and beetle pressure. Forest Ecology and Management 318: 158–166. https://doi.org/10.1016/j.foreco.2014.01.025

Kärvemo S., Rogell B., Schroeder M., 2014b. Dynamics of spruce bark beetle infestation spots: Importance of local population size and landscape characteristics after a storm disturbance. Forest Ecology and Management 334: 232–240. https://doi.org/10.1016/j.foreco.2014.09.011

Kärvemo S., Huo L., Öhrn P., Lindberg E., Persson H.J., 2023. Different triggers, different stories: Bark-beetle infestation patterns after storm and drought-induced outbreaks. Forest Ecology and Management 545: 121255. https://doi.org/10.1016/j.foreco.2023.121255

Kautz M., Dworschak K., Gruppe A., Schopf R., 2011. Quantifying spatio-temporal dispersion of bark beetle infestations in epidemic and non-epidemic conditions. Forest Ecology and Management 262: 598–608. https://doi.org/10.1016/j.foreco.2011.04.023

Lapin, M., Faško, P., Melo, M., Šťastný, P., Tomlain, J., 2002. Climatic regions. In: Landscape Atlas of the Slovak Republic, map 1:1 000 000, p. 94.

Lastovicka J., Svec P., Paluba D., Kobliuk N., Svoboda J., Hladky R., Stych P., 2020. Sentinel-2 data in an evaluation of the impact of the disturbances on forest vegetation. Remote Sensing 12: 1914. https://doi.org/10.3390/rs12121914

Lausch A., Fahse L., Heurich M., 2011. Factors affecting the spatio-temporal dispersion of *Ips typographus* (L.) in Bavarian Forest National Park: A long-term quantitative landscape-level analysis. Forest Ecology and Management 261: 233–245. https://doi.org/10.1016/j.foreco.2010.10.012

Lausch A., Heurich M., Gordalla D., Dobner H.-J., Gwillym-Margianto S., Salbach C., 2013. Forecasting potential bark beetle outbreaks based on spruce forest vitality using hyperspectral remote-sensing techniques at different scales. Forest Ecology and Management 308: 76–89. https://doi.org/10.1016/j.foreco.2013.07.043

Law K.H., Nichol J., 2004. Topographic correction for differential illumination effects on Ikonos satellite imagery. International Archives of Photogrammetry, Remote Sensing and Spatial Information Sciences 35: 641–646.

Leathwick J.R., Snelder T., Chadderton W.L., Elith J., Julian K., Ferrier S., 2011. Use of generalised dissimilarity modelling to improve the biological discrimination of river and stream classifications. Freshwater Biology 56: 21–38. https://doi.org/10.1111/j.1365-2427.2010.02414.x

Lillesand T., Kiefer R.W., Chipman J., 2015. Remote Sensing and Image Interpretation. 7th ed. Wiley, New York, 736 p.

Lindman L., Ranius T., Schroeder M., 2023. Regional climate affects habitat preferences and thermal sums required for development of the Eurasian spruce bark beetle, *Ips typographus.* Forest Ecology and Management 544: 121216. https://doi.org/10.1016/j.foreco.2023.121216

Marini L., Ayres M.P., Battisti A., Faccoli M., 2012. Climate affects severity and altitudinal distribution of outbreaks in an eruptive bark beetle. Climatic Change 115: 327–341. https://doi.org/10.1007/s10584-012-0463-z

Marini L., Lindelöw Å., Jönsson A.M., Wulff S., Schroeder L.M., 2013. Population dynamics of the spruce bark beetle: A long-term study. Oikos 122: 1768–1776. https://doi.org/10.1111/j.1600-0706.2013.00431.x

McCune B., Keon D., 2002. Equations for potential annual direct incident radiation and heat load index. Journal of Vegetation Science 13: 603–606. https://doi.org/10.1658/1100-9233(2002)013[0603:efpadi]2.0.co;2

Merzlyak M.N., Gitelson A.A., Chivkunova O.B., Rakitin V.Y., 1999. Non-destructive optical detection of pigment changes during leaf senescence and fruit ripening. Physiologia Plantarum 106: 135–141. https://doi.org/10.1034/j.1399-3054.1999.106119.x

Mezei P., Blaženec M., Grodzki W., Škvarenina J., Jakuš R., 2017. Influence of different forest protection strategies on spruce tree mortality during a bark beetle outbreak. Annals of Forest Science 74: 1–12. https://doi.org/10.1007/s13595-017-0663-9

Mezei P., Grodzki W., Blaženec M., Škvarenina J., Brandýsová V., Jakuš R., 2014. Host and site factors affecting tree mortality caused by the spruce bark beetle (*Ips typographus*) in mountainous conditions. Forest Ecology and Management 331: 196–207. https://doi.org/10.1016/j.foreco.2014.07.031

Mezei P., Potterf M., Škvarenina J., Rasmussen J.G., Jakuš R., 2019. Potential solar radiation as a driver for bark beetle infestation on a landscape scale. Forests 10: 604. https://doi.org/10.3390/f10070604

Migas-Mazur R., Kycko M., Zwijacz-Kozica T., Zagajewski B., 2021. Assessment of Sentinel-2 images, support vector machines and change detection algorithms for bark beetle outbreaks mapping in the Tatra Mountains. Remote Sensing 13(16): 3314. https://doi.org/10.3390/rs13163314

Mišurec J., Kopačková V., Lhoták̆ová Z., Campbell P., Albrechtová J., 2016. Detection of spatio-temporal changes of Norway spruce forest stands in Ore Mountains using Landsat time series and airborne hyperspectral imagery. Remote Sensing 8: 92. https://doi.org/10.3390/rs8020092

Müller M., Olsson P.-O., Eklundh L., Jamali S., Ardö J., 2022. Features predisposing forest to bark beetle outbreaks and their dynamics during drought. Forest Ecology and Management 523: 120480. https://doi.org/10.1016/j.foreco.2022.120480

Nardi D., Jactel H., Pagot E., Samalens J.-C., Marini L., 2023. Drought and stand susceptibility to attacks by the European spruce bark beetle: A remote sensing approach. Agricultural and Forest Entomology 25: 119–129. https://doi.org/10.1111/afe.12536

Negrón J.F., Cain B., 2019. Mountain pine beetle in Colorado: A story of changing forests. Journal of Forestry 117: 144–151. https://doi.org/10.1093/jofore/fvy032

Nilsson S.G., Nilsson I.N., 2004. Biodiversity in Linnaeus' birthplace in Småland 4: Vascular plants in Stenbrohults village. Svensk Botanisk Tidskrift 98: 65–150.

Økland B., Berryman A., 2004. Resource dynamic plays a key role in regional fluctuations of the spruce bark beetle *Ips typographus*. Agricultural and Forest Entomology 6: 141–146. https://doi.org/10.1111/j.1461-9555.2004.00214.x

Økland B., Nikolov C., Krokene P., Vakula J., 2016. Transition from windfall- to patch-driven outbreak dynamics of the spruce bark beetle Ips typographus. Forest Ecology and Management 363: 63–73. https://doi.org/10.1016/j.foreco.2015.12.007

Olofsson P., Foody G.M., Herold M., Stehman S.V., Woodcock C.E., Wulder M.A., 2014. Good practices for estimating area and assessing accuracy of land change. Remote Sensing of Environment 148: 42–57. https://doi.org/10.1016/j.rse.2014.02.015

Olofsson P., Foody G.M., Stehman S.V., Woodcock C.E., 2013. Making better use of accuracy data in land change studies: Estimating accuracy and area and quantifying uncertainty using stratified estimation. Remote Sensing of Environment 129: 122–131. https://doi.org/10.1016/j.rse.2012.10.031

Parisien M.A., Moritz M.A., 2009. Environmental controls on the distribution of wildfire at multiple spatial scales. Ecological Monographs 79: 127–154. https://doi.org/10.1890/07-1289.1

Parobeková Z., Sedmáková D., Kucbel S., Pittner J., Jaloviar P., Saniga M., Balanda M., Vencurik J., 2016. Influence of disturbances and climate on high-mountain Norway spruce forests in the Low Tatra Mts., Slovakia. Forest Ecology and Management 380: 128–138. https://doi.org/10.1016/j.foreco.2016.08.031

Potterf M., Nikolov C., Kočická E., Ferenčík J., Mezei P., Jakuš R., 2019. Landscape-level spread of beetle infestations from windthrown- and beetle-killed trees in the non-intervention zone of the Tatra National Park, Slovakia (Central Europe). Forest Ecology and Management 432: 489–500. https://doi.org/10.1016/j.foreco.2018.09.050

QGIS Development Team, 2021. QGIS Geographic Information System. Available at: https://qgis.org. Accessed 31 Jan 2022.

Ridgeway G., 2024. Generalized Boosted Models: A guide to the gbm package. CRAN vignette. https://cran.r-project.org/web/packages/gbm/

Rouse J.W., Haas R.H., Schell J.A., Deering D.W., Harlan J.C., 1974. Monitoring the vernal advancement and retrogradation (green wave effect) of natural vegetation. NASA Report No. E75-10354.

Schelhaas M.-J., Nabuurs G.-J., Schuck A., 2003. Natural disturbances in the European forests in the 19th and 20th centuries. Global Change Biology 9: 1620–1633. https://doi.org/10.1046/j.1365-2486.2003.00684.x

Seidl R., Schelhaas M.J., Lexer M.J., 2011. Unraveling the drivers of intensifying forest disturbance regimes in Europe. Global Change Biology 17: 2842–2852. https://doi.org/10.1111/j.1365-2486.2011.02452.x

Senf C., Seidl R., 2020. Mapping the forest disturbance regimes of Europe. Nature Sustainability 4: 63–70. https://doi.org/10.1038/s41893-020-00609-y

Senf C., Seidl R., 2018. Natural disturbances are spatially diverse but temporally synchronized across temperate forest landscapes in Europe. Global Change Biology 24: 1201–1211. https://doi.org/10.1111/gcb.13897

Siegfried J., Longchamps L., Khosla R., 2019. Multispectral satellite imagery to quantify in-field soil moisture variability. Journal of Soil and Water Conservation 74: 33–40. https://doi.org/10.2489/jswc.74.1.33

Stadelmann G., Bugmann H., Wermelinger B., Bigler C., 2014. Spatial interactions between storm damage and subsequent infestations by the European spruce bark beetle. Forest Ecology and Management 318: 167–174. https://doi.org/10.1016/j.foreco.2014.01.022

Trubin A., Kozhoridze G., Zabihi K., Modlinger R., Singh V.V., Surový P., Jakuš R., 2023. Detection of susceptible Norway spruce to bark beetle attack using PlanetScope multispectral imagery. Frontiers in Forests and Global Change 6: 1130721. https://doi.org/10.3389/ffgc.2023.1130721

Trubin A., Kozhoridze G., Zabihi K., Modlinger R., Singh V.V., Surový P., Jakuš R., 2024. Detection of green attack and bark beetle susceptibility in Norway Spruce: Utilizing PlanetScope Multispectral Imagery for Tri-Stage spectral separability analysis. Forest Ecology and Management, 560, p.121838. https://doi.org/10.1016/j.foreco.2024.121838

Weiss A.D., 2001. Topographic position and landforms analysis. In: Proceedings of the ESRI User Conference, San Diego, CA, USA.

Wermelinger B., 2004. Ecology and management of the spruce bark beetle *Ips typographus*—a review of recent research. Forest Ecology and Management 202: 67–82. https://doi.org/10.1016/j.foreco.2004.07.018

Wichmann L., Ravn H.P., 2001. The spread of *Ips typographus* (L.) (Coleoptera, Scolytidae) attacks following heavy windthrow in Denmark, analysed using GIS. Forest Ecology and Management 148: 31–39. https://doi.org/10.1016/S0378-1127(00)00477-1

Wulder M.A., Dymond C.C., White J.C., Leckie D.G., Carroll A.L., 2006. Surveying mountain pine beetle damage of forests: A review of remote sensing opportunities. Forest Ecology and Management 221: 27–41. https://doi.org/10.1016/j.foreco.2005.09.021

Xie Q., Dash J., Huang W., Peng D., Qin Q., Mortimer H., 2018. Vegetation indices combining the red and red-edge spectral information for leaf area index retrieval. IEEE Journal of Selected Topics in Applied Earth Observations and Remote Sensing 11: 1482–1492. https://doi.org/10.1109/JSTARS.2018.2813281

Young D.J.N., Slaton M.R., Koltunov A., 2023. Temperature is positively associated with tree mortality in California subalpine forests containing whitebark pine. Ecosphere 14(2): e4400. https://doi.org/10.1002/ecs2.4400

Zhong L., Hu L., Zhou H., 2019. Deep learning based multi-temporal crop classification. Remote Sensing of Environment 221: 430–443. https://doi.org/10.1016/j.rse.2018.11.032

R Core Team, 2020. R: A language and environment for statistical computing. R Foundation for Statistical Computing, Vienna. Available at: https://www.R-project.org/

XGBoost Developers, 2024. Introduction to Boosted Trees – XGBoost 1.7.6 documentation. Available at: https://xgboost.readthedocs.io/en/stable/tutorials/model.html